

## Modelling of Schiff Base Vanillin Derivatives Targeting *Streptococcus Pneumoniae* Bacterial Neuraminidase

WOON YI LAW\* & MOHD RAZIP ASARUDDIN

Department of Chemistry, Faculty of Resource Science and Technology, Universiti Malaysia Sarawak, 94300 Kota Samarahan, Sarawak, Malaysia

\*Corresponding author: [mendah\\_wylaw@hotmail.com](mailto:mendah_wylaw@hotmail.com)

Received: 21 November 2024

Accepted: 21 May 2025

Published: 31 December 2025

### ABSTRACT

*Streptococcus pneumoniae* is a pathogenic bacterium which has led to serious pneumococcal infections. Despite the fact that efficient therapeutic agents and vaccinations are available for the treatment of *Streptococcus pneumoniae* infections, more strains of *Streptococcus pneumoniae* have acquired significant resistance towards the available antibiotics. The neuraminidase of *Streptococcus pneumoniae* possess significant contribution in pathogenesis, aiding the release and spread of virus. Simultaneously, Schiff base vanillin derivatives were reported in past literature for their great deal of potential as inhibitors of influenza virus neuraminidase. Hence, the research aims to evaluate the inhibitory activity of Schiff base vanillin derivatives against *Streptococcus pneumoniae* neuraminidase via ligand-based pharmacophore modelling and structure-based molecular docking using LigandScout 4.4.9 and AutoDock 4.2. Ligand-based pharmacophore modelling was performed to analyse the anti-neuraminidase activity of Schiff base vanillin derivatives based on their pharmacophore fit values and matching pharmacophore features with a pharmacophore model, generated from a list of training sets, which are reported drugs against *Streptococcus pneumoniae* neuraminidase. In structure-based molecular docking, the Schiff base vanillin derivatives were evaluated based on their docking performances with the active sites of the crystal structure of PDB:2YA8. Evaluations were based on their pharmacophore scores, binding affinity and matching interactions with the inhibitory ligand of 2YA8. 20 out of 21 Schiff base vanillin derivatives successfully show good results in ligand-based pharmacophore modelling, as well as satisfying docking performances in structure-based molecular docking. Furthermore, they also fulfill the Lipinski's Rule of 5, thus displaying appreciable potential as inhibitors of *Streptococcus pneumoniae* neuraminidase.

**Keywords:** Molecular docking, neuraminidase, pharmacophore modelling, Schiff base vanillin derivatives, *Streptococcus pneumoniae*

Copyright: This is an open access article distributed under the terms of the CC-BY-NC-SA (Creative Commons Attribution-NonCommercial-ShareAlike 4.0 International License) which permits unrestricted use, distribution, and reproduction in any medium, for non-commercial purposes, provided the original work of the author(s) is properly cited.

### INTRODUCTION

Pneumococcal infections are any infections caused by the bacteria *Streptococcus pneumoniae*, also known as pneumococcus, as shown in Figure 1. The bacteria commonly reside in the human upper respiratory tract, nasal cavity and sinuses (World Health Organization, 2022). As a pathogenic bacterium, it has caused significant morbidity and mortality all over the world, especially among the children and elder people in developing areas (Lv *et al.*, 2020). *Streptococcus pneumoniae* is alpha-hemolytic, which means that it is able to produce hydrogen peroxide (H<sub>2</sub>O<sub>2</sub>) which oxidizes hemoglobin

within the erythrocytes. The presence of H<sub>2</sub>O<sub>2</sub> may lead to destruction of DNA and apoptosis of lung cells (Oliver, 2019). On top of that, for inhabiting human nasopharynx asymptotically, it has led to numerous invasive pneumococcal infections, such as pneumonia, meningitis, otitis media and bacteremia (Nguyen & Bhattacharya, 2022). The infections were responsible for at least 1-2 million infant deaths all over the world (Bogaert *et al.*, 2004), and before the development and availability of antibiotics, about 95% of the cases of pneumonia were caused by *Streptococcus pneumoniae* (Dion & Ashurst, 2022).

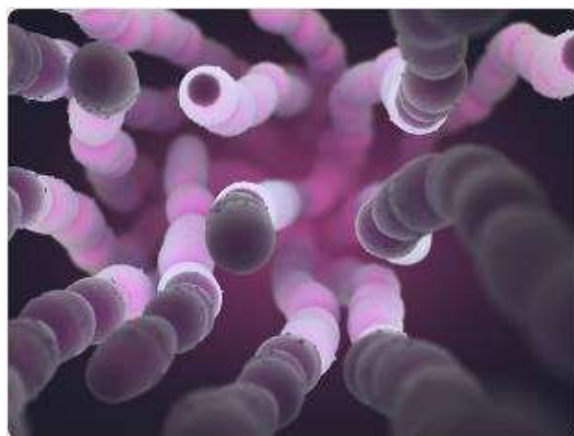


**Figure 1.** *Streptococcus pneumoniae* (Oliver, 2019)

Pneumococcal infections can affect all age groups, but children younger than 2 years old and senior citizens who are 65 years old and above possess a higher risk of infection (European Centre for Disease Prevention and Control, 2023). Apart from that, patients with health conditions that may lead to immune deficits such as diabetes mellitus and HIV infections, as well as health conditions associated with decreased pulmonary clearance functions such as asthma, chronic bronchitis, or chronic obstructive pulmonary disease are also at higher risk (Iyer & Perloff, 2023). There are many *Streptococcus pneumoniae* serotypes being discovered, however only a few of them are responsible for most of the serious and invasive infections (European Centre for Disease Prevention and Control, 2023). Based on the epidemiological surveillance of *Streptococcus pneumoniae* infections within the Malaysian population carried out by the Bacteriology Division of the Institute for Medical Research (IMR) from 1994 to 1995, out of 273 *Streptococcus pneumoniae* isolations from different clinical samples, most of them belong to only 5 serotypes, which were serotypes 1, 6B, 19B, 19F and 23F (Rohani *et al.*, 1999). Back then in the 1990s, *Haemophilus influenzae* type b vaccine successfully decreases the invasive Hib infections in most of the European countries, but on the other hand causing *Streptococcus pneumoniae* to become the leading outbreak of meningitis and sepsis among children (European Centre for Disease Prevention and Control, 2023). Thereupon, vaccines for pneumococcal infections have been developed to overcome the situation. The introduction of 7-valent Pneumococcal Conjugate Vaccine (PCV 7) has successfully altered the epidemiology of

pneumococcal infections in many countries, in which pneumococcal infections had decrease by 94% in the United States (European Centre for Disease Prevention and Control, 2023). Other pneumococcal conjugate vaccines include PCV13, PCV15, and PCV20, as well as pneumococcal polysaccharide vaccine (PPSV23) (Centers for Disease Control and Prevention, 2023). Antibiotics have been prescribed as the main treatment for *Streptococcus pneumoniae* infections. The commonly used antibiotics include penicillin, macrolides, clindamycin, cephalosporin, rifampin, vancomycin, and trimethoprim-sulfamethoxazole, which were utilized until the 70s (Iyer & Perloff, 2023). Other than that, amoxicillin is given to patients with pneumonia, otitis media and sinusitis (Musher, 2019). Despite significant studies, developments and availability of effective therapeutic agents and vaccines, the mortality rate has remained high due to the increasing number of strains that are resistant to the available antibiotics which complicates the medications (Lv *et al.*, 2020). Due to antibiotic abuse in hospitals, multidrug-resistant and vancomycin-resistant strains have drastically increased, with 15 - 30% of the pneumococcal strains being multi-drug resistant (Li *et al.*, 2009). It was reported by Centers of Disease Control and Prevention (CDC) that up to 40% of the pneumococcal infections until 2000 were due to resistance of pneumococcal bacteria to at least one type of antibiotic (Centers for Disease Control and Prevention, 2024). For the increasing emergence of antibiotic-resistance *Streptococcus pneumoniae* isolates, the greater increase of more serious and risky complications may be a possible concern in the future.

*Streptococcus pneumoniae* possesses a number of virulence factors which plays an important role in infection, which are capsules, pneumolysin, sortase A, pneumococcal surface protein A, hyaluronidase and neuraminidase (Maragakis *et al.*, 2008). A great deal of research was performed to discover and develop drugs, natural compounds or novel compounds based on their inhibitory activity against these proteases. For instance, quercetin, polyhydroxy flavonoid compound which is found in the leaves, fruits and flowers of plants, was found out to be able to inhibit pneumolysin via hemolysis assay and oligomerization assay (Nguyen & Bhattacharya, 2022). Interestingly, honeys from Malaysia origin were found out to be able to inhibit hyaluronidase of *Streptococcus pneumoniae*, with honeys from Kelulut to be reported for its highest inhibitory activity against hyaluronidase (Nayian & Yusof, 2020). Other than inhibiting the proteases, another research reported the *in silico* discovery of 6 novel compounds, 1 from imidazole analogue, 4 from furan derivatives and 1 from thiophene derivative, being able to inhibit the histidine kinase (HK) VicK protein, which is important for the growth of bacterium (Li *et al.*, 2009).

Neuraminidase A of *Streptococcus pneumoniae*, NanA, played an imperative role by catalyzing the release and removal of terminal sialic acid residues from cell membrane glycostructures, hence decreasing the binding of complement regulator factor H to cell surfaces (Parker *et al.*, 2009; Syed *et al.*, 2019). There were three homologous neuraminidase encoded: NanA, NanB and NanC, based on different sequence of amino acids, choice of substrates and types of reactions. The specific roles of the three neuraminidases were still not completely discovered, however, NanA was confirmed for its significant importance in pathogenesis (Sharapova *et al.*, 2018). Nonetheless, research related to the findings of drugs or inhibitors against *Streptococcus pneumoniae* neuraminidase were very limited and inadequate. This is because most of the research related to the search of *Streptococcus pneumoniae* neuraminidase were at the early stages of study, such as the search of prenylated flavonoids against neuraminidase of both influenza virus and *Streptococcus pneumoniae* (Grienke *et al.*, 2016). Additionally, most of the research focuses on the study of influenza virus neuraminidase inhibitors. Chlorogenic acid was

reported to show strong inhibitory activity against neuraminidase of influenza virus, but inhibitory activity against neuraminidase of *Streptococcus pneumoniae* was still considered limited (Guan *et al.*, 2020). Hence, it has been a great interest and potential in research of development and findings of compounds that possess inhibitory activity against neuraminidase of *Streptococcus pneumoniae*.

Schiff base vanillin derivatives are compounds derived from the Schiff base synthesis reaction between vanillin and primary amines. Previously, a research has reported that neuraminidase of influenza virus was able to be inhibited by Schiff base vanillin derivatives, compounds derived from the Schiff base synthesis mechanism between vanillin and primary amines, by *in silico* pharmacophore modelling, virtual screening and molecular docking, as well as via 2'-(4-Methylumbelliferyl)- $\alpha$ -D-N-acetylneuraminic acid (MUNANA) assay (Asaruddin, 2016). This raises a great interest and potential as the viral neuraminidase and bacterial neuraminidase play the same role by cleaving sialic acid residues from cell surfaces and facilitates the release and spread of virus from infected cells (Benton *et al.*, 2017). Thereupon, the research focuses on the inhibitory activity of Schiff base vanillin derivatives against neuraminidase of *Streptococcus pneumoniae*. This study is done by performing *in silico* screenings, which include ligand-based pharmacophore modellings and structure-based molecular dockings.

## MATERIALS & METHODS

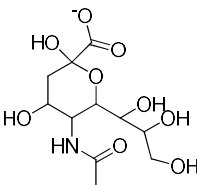
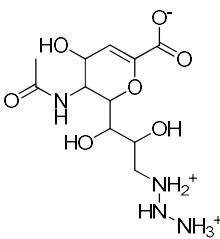
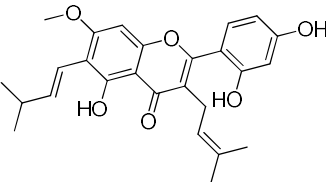
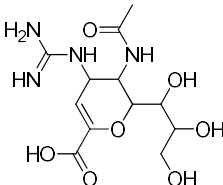
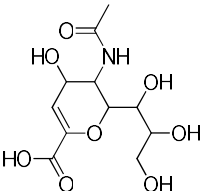
### Pharmacophore Model Preparation

Preparation of pharmacophore model was done by using LigandScout 4.4.9 software. A list of chemical compounds with diverse chemical structures that were reported for their inhibitory activity against neuraminidase of *Streptococcus pneumoniae* were selected as training sets to generate a pharmacophore model for the evaluation of Schiff base vanillin derivatives as inhibitors of *Streptococcus pneumoniae* neuraminidase. The chemical structures of the training sets were initially drawn by using ChemDraw Ultra 12.0 and downloaded in the MDL-mol file formats. The training sets include zanamivir (Gut *et al.*, 2011), atorcarpin (Walther *et al.*, 2015), DANA (2-deoxy-2,3-dehydro-N-

acetyl-neuraminic acid) (Owen *et al.*, 2015), NANA (N-acetyl-alpha-neuraminic acid) (Hsiao *et al.*, 2009) and 9N3Neu5Ac2e (5-acetamido-2,6-anhydro-3,5,9-trideoxy-9-triazan-1-yl-D-glycero-D-galacto-non-2-enonic acid). They

were later imported into the ligand-based perspective of LigandScout 4.4.9. Table 1. shows the chemical structures of training sets used to generate pharmacophore model.

**Table 1.** Chemical structures of training sets used to generate pharmacophore model

Name of training sets	Chemical structures
NANA (N-acetyl-alpha-neuraminic acid)	
9N3Neu5Ac2e (5-acetamido-2,6-anhydro-3,5,9-trideoxy-9-triazan-1-yl-D-glycero-D-galacto-non-2-enonic acid)	
Artocarpin	
Zanamivir	
DANA (2-deoxy-2,3-dehydro-N-acetyl-neuraminic acid)	

Based on Table 1, NANA, DANA and 9N3Neu5Ac2e are sialic acid residues, zanamivir is a synthetic neuraminidase inhibitor, whereas artocarpin is a natural isoprenylated flavone. Due to their diverse chemical structures and different nature, they were able to generate a good pharmacophore model which account for

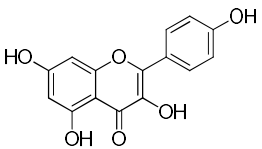
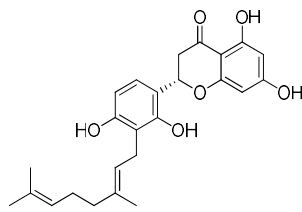
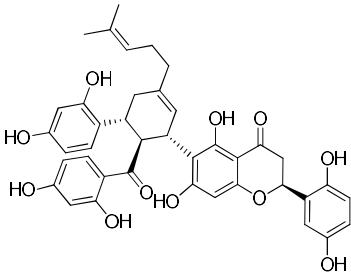
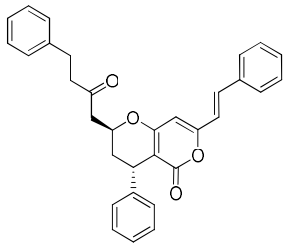
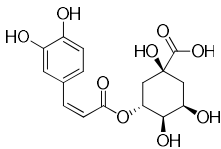
different binding interactions with the neuraminidase of *Streptococcus pneumoniae*.

The generated pharmacophore model is validated for its reliability by analysis with a list of test sets. Therefore, a list of chemical compounds from natural products which were previously reported to exhibit inhibitory activity

against *Streptococcus pneumoniae* neuraminidase were selected as test sets to perform such validation. The 2D structure of the chemical structures of the test sets were also drawn by using ChemDraw Ultra 12.0, downloaded in the MDL-mol file format and imported into the ligand-based perspective of LigandScout 4.4.9 together with the list of training sets. Due to limited studies, the natural products available to be selected as test sets in literature review were also limited. Based on literature study, the test sets that were reported for their strong and affirm inhibitory activity

against *Streptococcus pneumoniae* neuraminidase include kaempferol (Xu *et al.*, 2023), Sanggenol A, Sanggenon G (Grienke *et al.*, 2016), Katsumadain A (Walther *et al.*, 2015) and chlorogenic acid (Guan *et al.*, 2020), with chemical structures as depicted in Table 2. Not only due to the reported literature review, the test sets were all greatly diverse chemical structures among themselves and in comparison with training sets. This provides further fundamental support to confirm the reliability of the generated pharmacophore model due to their different chemical properties.

**Table 2.** Chemical structures of test sets to validate the reliability of generated pharmacophore model

Name of test sets	Chemical structures
Kaempferol	
Sanggenol A	
Sanggenon G	
Katsumadain A	
Chlorogenic acid	

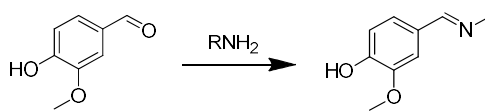
When all MDL-mol files of training and test sets were imported, the MMFF94 energy of the chemical structures were minimised to reach the closest local minimum. Conformations of the ligand sets were generated by using the FAST settings, and the ligand sets were clustered based on pharmacophore RDF-code similarity and average cluster distance calculation. Subsequently, ligand-based pharmacophore modelling was run based on pharmacophore fit scoring function, and the pharmacophore model was generated based on merged pharmacophore feature. The evaluation of the generated model was based on matching pharmacophore features, model scores and pharmacophore fit values depicted by training sets and test sets. If the test sets were able to depict more than half of the matching features and fit values of the training sets, then the generated pharmacophore model is said to be reliable for evaluation of potential inhibitory activity against *Streptococcus pneumoniae* neuraminidase. Additionally, the root mean square deviation (RMSD) values of

the test sets in alignment with the pharmacophore model, as well as their cosine similarities were also evaluated to further validate the reliability of the generated pharmacophore model.

### Ligand-based Pharmacophore Modelling of Schiff Base Vanillin Derivatives

A total of 21 Schiff base vanillin derivatives were selected to be evaluated for their inhibitory activity against *Streptococcus pneumoniae* neuraminidase. The chemical structures of these compounds were drawn using ChemDraw Ultra 12.0, downloaded in the MDL-mol file format and imported as test sets in the generated pharmacophore model. The general synthetic route of Schiff base vanillin derivatives was as illustrated in Figure 2.

The chemical structures of the primary amines and the Schiff base vanillin derivatives are as shown in Table 3.

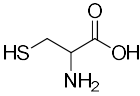
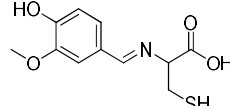
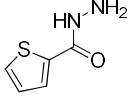
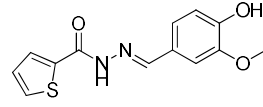
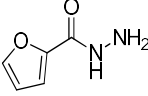
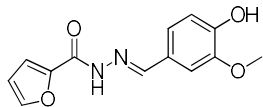
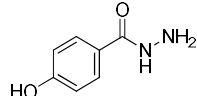
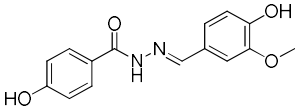
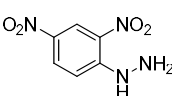
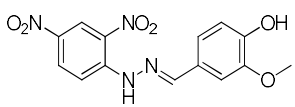
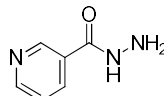
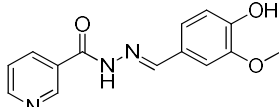
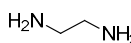
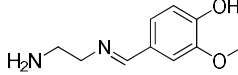
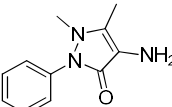
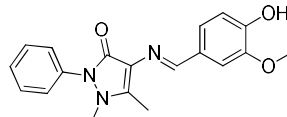
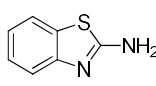
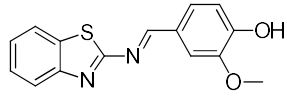
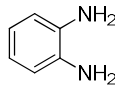
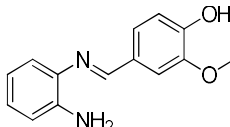
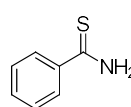
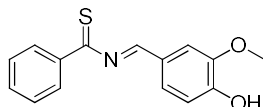
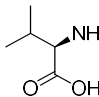
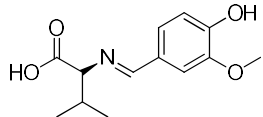
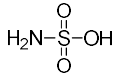
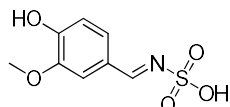


**Figure 2.** General synthetic route of Schiff base vanillin derivatives

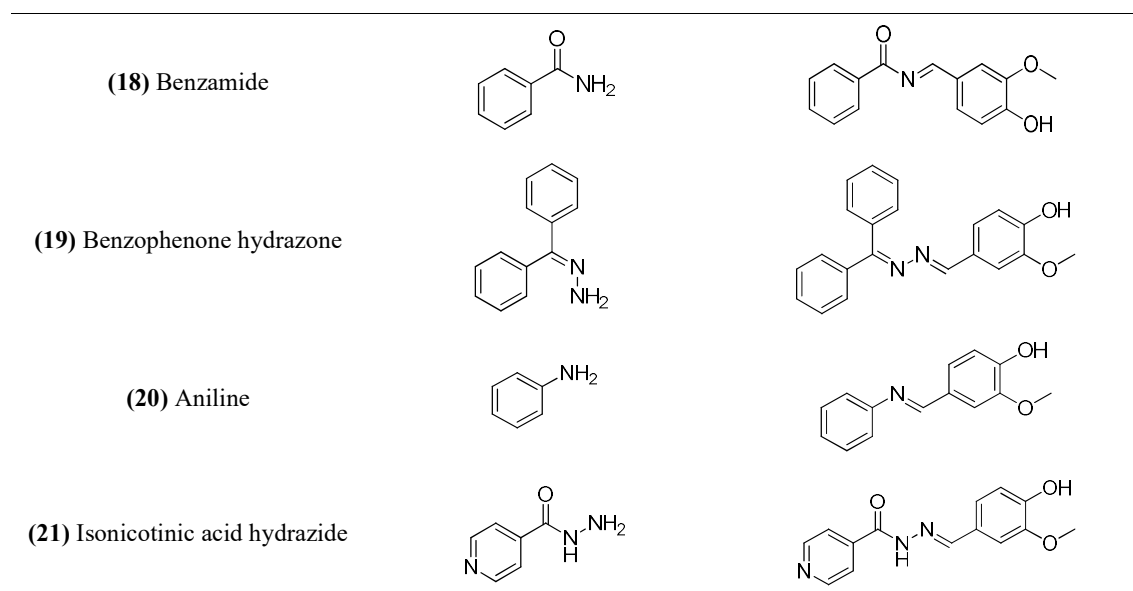
**Table 3.** Chemical structures of primary amines and resulting Schiff base vanillin derivatives

Name of primary amines	Chemical structures of primary amine	Schiff base vanillin derivatives
(1) Salicyl hydrazide		
(2) Serine		
(3) Hydrazide hydrate	$\text{H}_2\text{N}-\text{NH}_2$ $\text{H}-\text{O}-\text{H}$	
(4) Phenylhydrazine		

---

(5) Cysteine		
(6) 2-thiophene carboxylic acid hydrazide		
(7) 2-furoic acid hydrazide		
(8) 4-hydroxybenzhydrazide		
(9) 2,4-dinitrophenylhydrazine		
(10) Nicotinic hydrazide		
(11) Ethylenediamine		
(12) 4-aminoantipyrine		
(13) 2-aminobenzothiazole		
(14) O-phenyldiamine		
(15) Thiobenzamide		
(16) L-valine		
(17) Sulfamic acid		

---



After the import of Schiff base vanillin derivatives as test sets, similarly, MMFF94 energies of all datasets were minimised. Conformations of the ligand sets were generated, and the ligand sets were clustered based on pharmacophore RDF-code similarity and average cluster distance calculation. Ligand-based pharmacophore modelling was run and the Schiff base vanillin derivatives were analysed for their potential inhibitory activity against *Streptococcus pneumoniae* neuraminidase based on their matching pharmacophore features and fit values with the generated pharmacophore model. Schiff base vanillin derivatives that were able to depict satisfied results in ligand-based pharmacophore modelling were later subjected to structure-based molecular docking for further assessment.

### Molecular Docking

The crystal structure of *Streptococcus pneumoniae* neuraminidase A, NanA (TIGR4) in complex with oseltamivir carboxylate (PDB code: 2YA8), as shown in Figure 3., was first retrieved from Protein Data Bank (PDB), and imported into the structure-based perspective of LigandScout 4.4.9. The oseltamivir carboxylate is the inhibitory ligand in the active site of the crystal structure as shown in Figure 4. and Figure 5., which possess inhibitory activity against *Streptococcus pneumoniae* neuraminidase. Hence, the Schiff base vanillin derivatives were evaluated based on their alignment with the pharmacophore model of the oseltamivir carboxylate ligand, as well as the protein-ligand interaction in the active site *via* molecular docking of the vanillin derivatives in the active site of 2YA8.

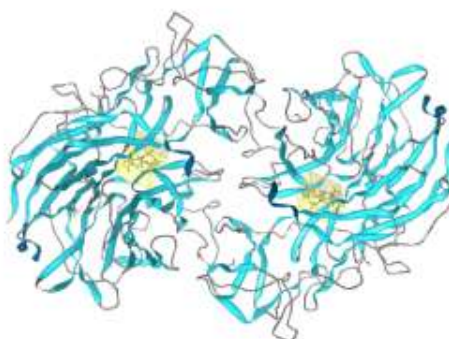


**Figure 3.** Crystal structure of *Streptococcus pneumoniae* neuraminidase A in complex with oseltamivir carboxylate (2YA8)



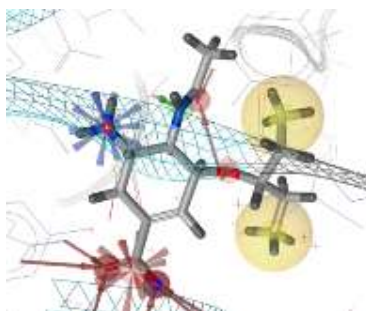


**Figure 4.** Pharmacophore model of the ligand, oseltamivir carboxylate in the active site of 2YA8

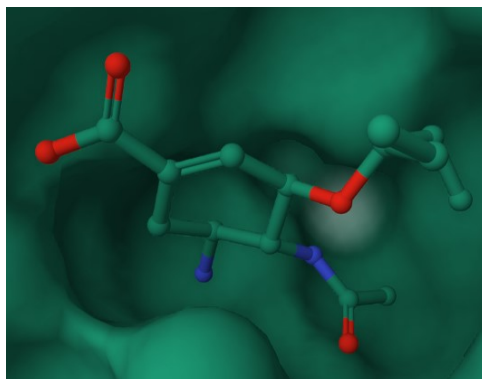


**Figure 5.** Illustration of oseltamivir carboxylate ligand in the active site of 2YA8

All Schiff base vanillin derivatives were first converted to the MDL-sdf file formats by using Open Babel GUI 2.3.1. They were imported one at a time into the alignment perspective of LigandScout 4.4.9 together with the pharmacophore model and ligand structure of oseltamivir carboxylate. In the alignment

perspective, beginning from the first Schiff base vanillin derivative, alignment was performed to oseltamivir carboxylate. Upon successful alignments, common pharmacophore features between both chemical structures were analysed as shown in Figure 6, depicted by the orange spots.

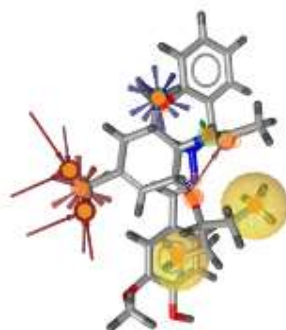


**Figure 6.** Successful alignment between Schiff base vanillin derivative and oseltamivir carboxylate

Based on the common features shared between the two structures, a shared pharmacophore model was generated, and the pharmacophores were merged, followed by interpolation of overlapping features. All ligands and pharmacophore models were injected into

the active site of 2YA8. Interactions shown by the Schiff base vanillin derivatives towards the active site of 2YA8 were analysed and compared with the oseltamivir carboxylate ligand, with an example as depicted in Figure 7.

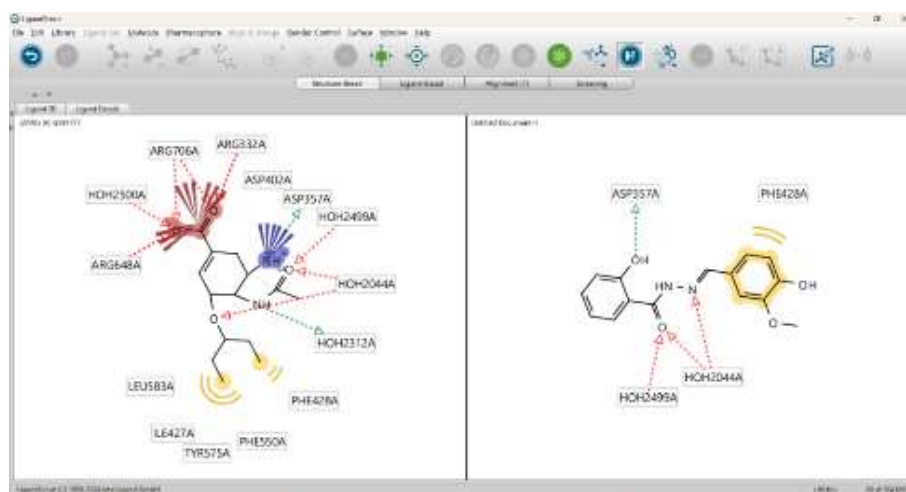


**Figure 7.** Interactions depicted by the vanillin derivative in the active site of 2YA8 in comparison with oseltamivir carboxylate ligand

The binding affinities of all Schiff base vanillin derivatives were determined by docking using AutoDock 4.2. Schiff base vanillin derivatives that successfully show good alignment with the oseltamivir carboxylate ligand, interactions with the active site of 2YA8, as well as good binding affinity and pharmacophore scores were recorded.

### Druglikeness Evaluation

Schiff base vanillin derivatives that successfully showed good results in ligand-based pharmacophore modelling and structure-based molecular docking were evaluated for their druglikeness properties based on Lipinski's Rule of 5 (RO5). The vanillin derivatives were considered potential orally active drugs if they possess not more than 5 hydrogen bond donors (HBD) (nitrogen-hydrogen and oxygen-hydrogen bonds), not more than 10 hydrogen

bond acceptors (HBA) (nitrogen and oxygen atoms), molecular weight less than 500 g/mol and partition coefficient log P not greater than 5 (Benet *et al.*, 2016).

## RESULTS & DISCUSSION

### Generation and Validation of Pharmacophore Model in Ligand-based Pharmacophore Modelling

A pharmacophore model was successfully generated by the 5 training sets. The training sets depicted pharmacophore fit values ranging from 74.09 to 98.79 in the generated model, which is considerably high. The model is made up of 10 common pharmacophore features, which is composed of 5 hydrogen bond acceptors (HBA) and 5 hydrogen bond donors (HBD). The generated model is as illustrated in Figure 8.

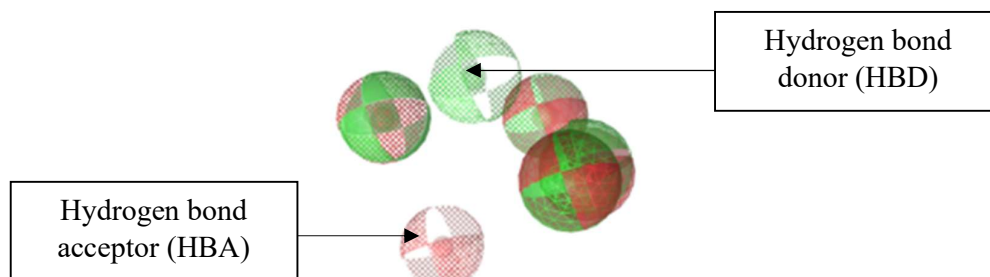


**Figure 8.** Generated pharmacophore model by training sets

Upon validation of the model by test sets, all test sets successfully depict good pharmacophore fit values in the generated model, ranging from 46.79 to 90.43, which is

more than half of the fit values shown by training sets. On top of that, out of the 10 common pharmacophore features, the test sets were able to show good alignment with 4 to 9 features, thus

depicting satisfying matching alignment. On top of that, chlorogenic acid, sanggenol A and sanggenon G even showed pharmacophore fit values higher than a few training sets, depicting good matching result. Katsumadain A showed lower pharmacophore fit values than the rest of the test sets, which may be due the lack of hydroxyl groups compared to other test sets, as well as larger chemical structure which may not fit in the pharmacophore model well.

On top of that, the RMSD value further affirm the reliability of the pharmacophore model. Theoretically, an RMSD value less than 2 Å is considerably good, but the lower the RMSD value, the better the agreement of the pharmacophore model with the actual binding pose (Al-Shar'i & Musleh, 2020). It was concluded that all 5 test sets were able to show RMSD value less than 1.5 Å. This provides further fundamental support to the validation of the reliability of the pharmacophore model.

Cosine similarity is a mathematical method utilized to measure the similarity values between two vectors. By measuring the similarity values between a pharmacophore model and the pharmacophore features of the test sets, the reliability of the pharmacophore model can be further affirmed. Based on the values ranging from -1 to 1, cosine similarities from 0 to 1 indicate strong similarity between the pharmacophore model and the test sets (Neela & Peram, 2025). Cosine similarities were

calculated by using the formula, Eq. (1) as shown:

$$\text{Cosine similarity} = \cos \theta = \frac{A \cdot B}{\|A\| \cdot \|B\|} \quad \text{Eq. (1)}$$

where  $A \cdot B$  = Dot product of vectors A and B











A = magnitude of vector A  
(pharmacophore model)

B = magnitude of vector B (test set)

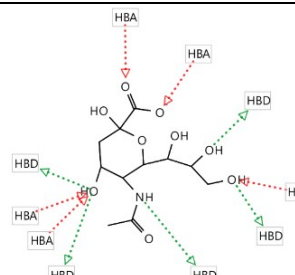
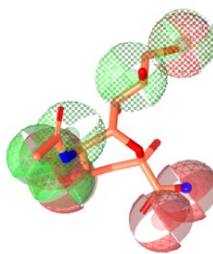
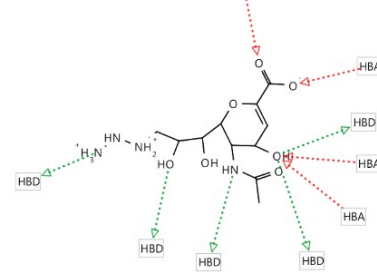
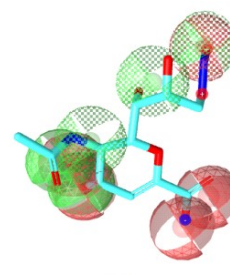
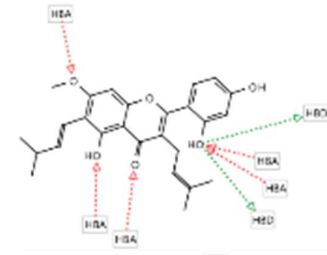
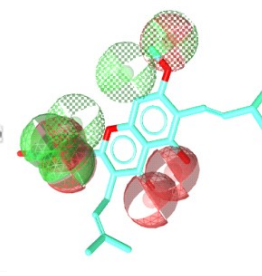
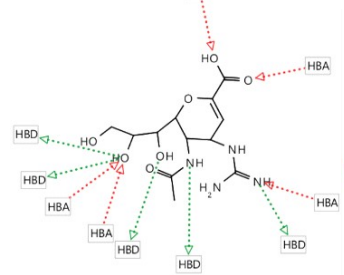
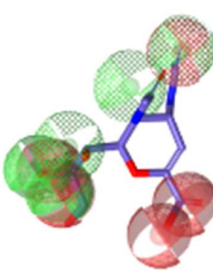
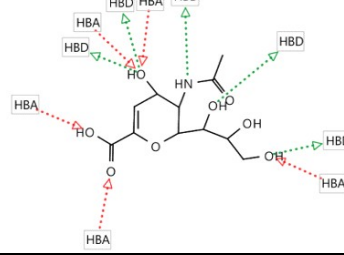
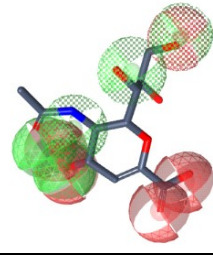
By calculating cosine similarities with pharmacophore vector of [5, 5, 0, 0, 0] due to 5 HBA and 5 HBD in the model, all 5 test sets were able to show cosine similarity values in between 0 and 1, showing strong similarity with the pharmacophore model. This further validate the reliability of the generated pharmacophore model.

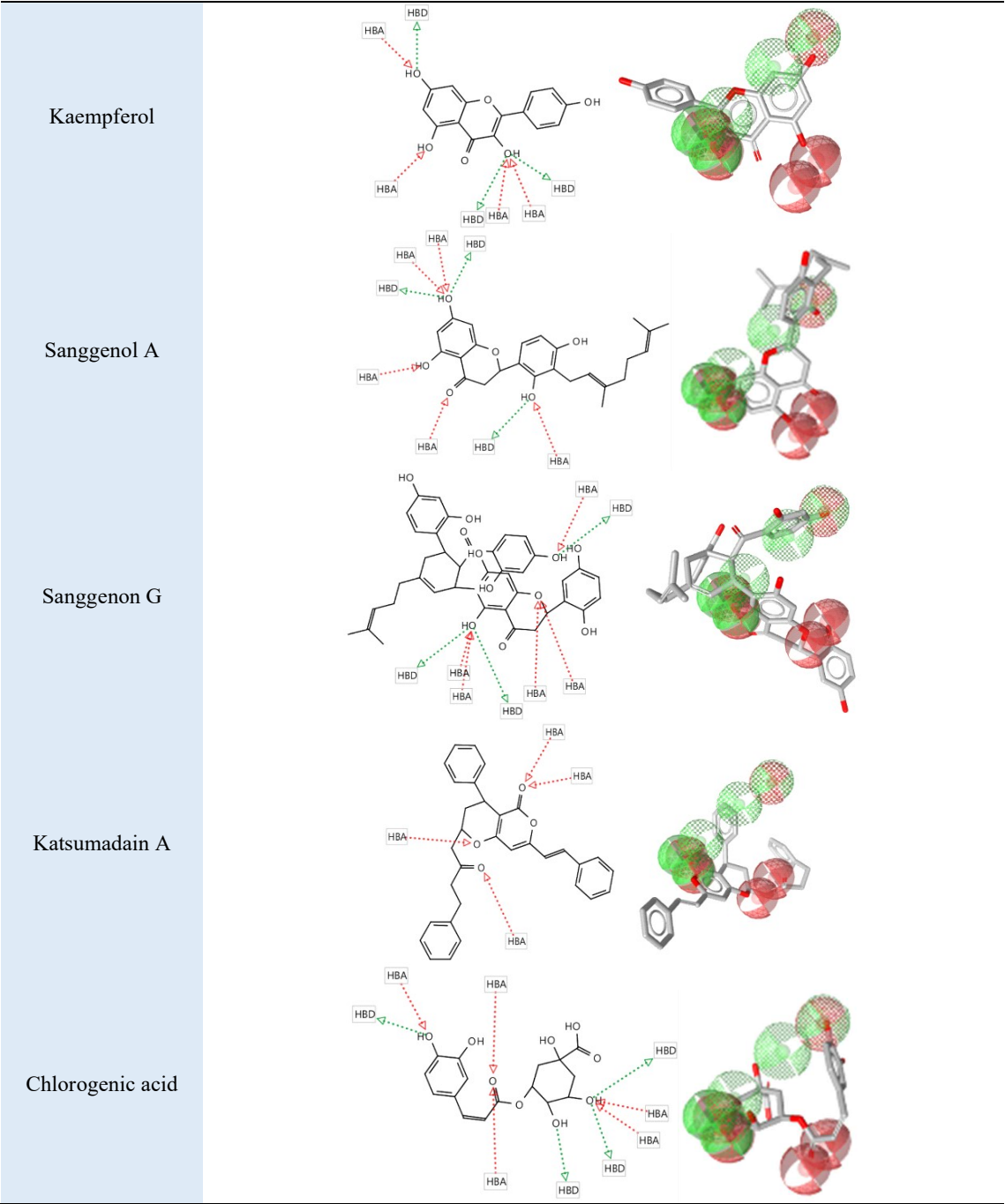
As a whole, the generated pharmacophore model was said to be validated for its reliability as model for evaluation of Schiff base vanillin derivatives as potential inhibitors against neuraminidase of *Streptococcus pneumoniae*. The overall matching features and pharmacophore fit values of training and test sets in the model were shown in Table 4. The matching features shown by respective functional groups of the chemical structures of Schiff base vanillin derivatives were shown in Table 5, the RMSD-based evaluation of test sets alignment to the pharmacophore model was shown in Table 6, whereas the cosine similarities of test sets and the pharmacophore model was as illustrated in Table 7.

**Table 4.** Matching features and pharmacophore fit values of training sets and test sets in the pharmacophore model, and RMSD values of test sets

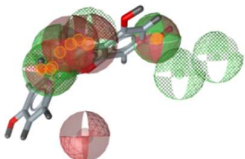
Training sets	Matching features	Pharmacophore fit values
Test sets		
NANA		98.59
9N3Neu5Ac2e		90.28
Artocarpin		74.09
Zanamivir		98.27
DANA		98.79
Kaempferol		72.02
Sanggenol A		82.28
Sanggenon G		82.65
Katsumadain A		46.79
Chlorogenic acid		90.43

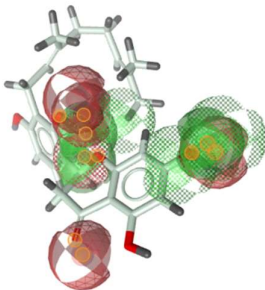
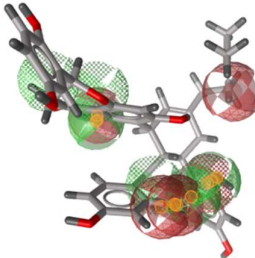
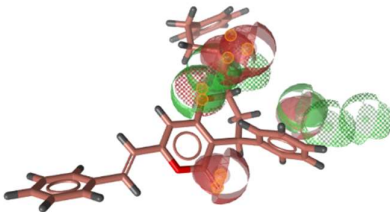
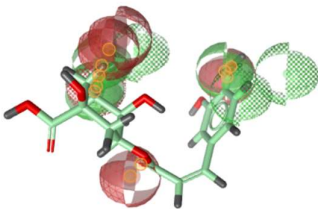
**Table 5.** Matching features shown by respective functional groups of Schiff base vanillin derivatives

Training sets	Matching features	
Test sets		
NANA		
		
		
		
		



**Table 6.** RMSD-based evaluation of test sets alignment to the pharmacophore model

Test sets	Alignment of test sets with pharmacophore model	RMSD values
Kaempferol		0.835

Sanggenol A		1.219
Sanggenon G		0.546
Katsumadain A		1.052
Chlorogenic acid		0.932

**Table 7.** Cosine similarities of test sets and pharmacophore model

Test sets	Vector of test sets	Cosine similarity
Kaempferol	[1, 6, 2, 0, 0]	0.77
Sanggenol A	[2, 3, 2, 1, 0]	0.83
Sanggenon G	[1, 2, 3, 1, 0]	0.55
Katsumadain A	[1, 4, 2, 1, 0]	0.75
Chlorogenic acid	[2, 5, 1, 0, 0]	0.90

#### Analysis of Schiff Base Vanillin Derivatives as Potential Neuraminidase Inhibitors of *Streptococcus Pneumoniae* in Ligand-based Pharmacophore Modelling

It was found out that out of all 21 Schiff base vanillin derivatives, compounds (1) to (10) were able to show good matching features and pharmacophore fit values greater than 70 in the generated pharmacophore model. Compounds (11) to (21) showed slightly lowered pharmacophore fit values and less optimal fit.

This is greatly due to the lack of proper functional groups to fit in the pharmacophore model, thus lack of suitable molecular structure. This can be explained by the depiction of pharmacophore features. Out of 10 pharmacophore features depicted by the pharmacophore model, compounds (1) to (10) successfully depicted 7 to 8 pharmacophore features, whereas compounds (11) to (21) depicted 6 pharmacophore features. Additionally, it was also noted that 2 derivatives show fit values higher than one of the training



sets, therefore having great potential as neuraminidase inhibitors of *Streptococcus pneumoniae*. Table 8 shows the matching features and pharmacophore fit values of the list of Schiff base vanillin derivatives in the pharmacophore model, arranged in descending

order of pharmacophore fit values and number of matching features. Table 9 shows the matching features depicted by respective functional groups of the chemical structures of Schiff base vanillin derivatives in the pharmacophore model.

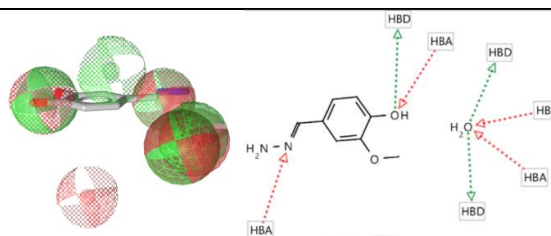
**Table 8.** Matching features and pharmacophore fit values of the list of Schiff base vanillin derivatives in the pharmacophore model

Schiff base vanillin derivatives	Matching features	Pharmacophore fit values
(1) Salicyl hydrazide		81.50
(2) Serine		81.31
(3) Hydrazide hydrate		74.49
(4) Phenylhydrazine		74.42
(5) Cysteine		74.35
(6) 2-thiophene carboxylic acid hydrazide		74.20
(7) 2-furoic acid hydrazide		74.16
(8) 4-hydroxybenzhydrazide		74.12
(9) 2,4-dinitrophenylhydrazine		73.99
(10) Nicotinic hydrazide		73.29
(11) Ethylenediamine		65.81
(12) 4-aminoantipyrine		64.68
(13) 2-aminobenzothiazole		64.61
(14) O-phenylenediamine		64.61
(15) Thiobenzamide		64.58
(16) L-Valine		64.56
(17) Sulfamic acid		64.56
(18) Benzamide		64.56
(19) Benzophenone hydrazine		64.55
(20) Anilline		64.54
(21) Isonicotinic acid hydrazide		64.25

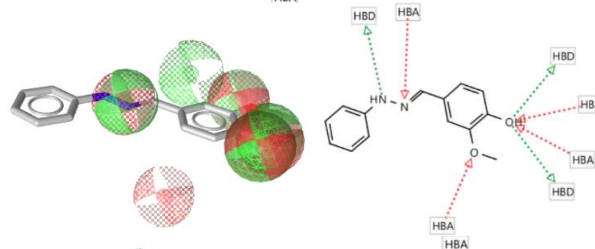
**Table 9.** Matching features depicted by respective functional groups of Schiff base vanillin derivatives

Schiff base vanillin derivatives (Vanillin + ...)	Matching features
(1) Salicyl hydrazide	
(2) Serine	

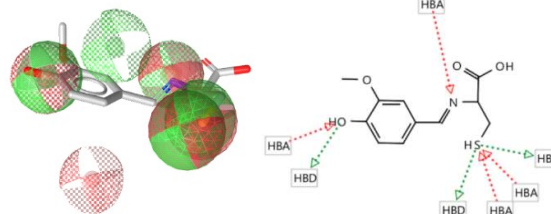
(3) Hydrazone hydrate



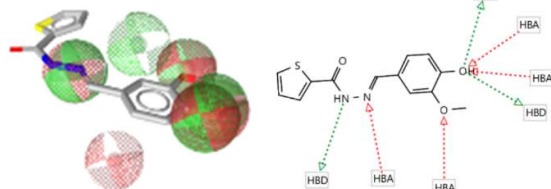
(4) Phenylhydrazine



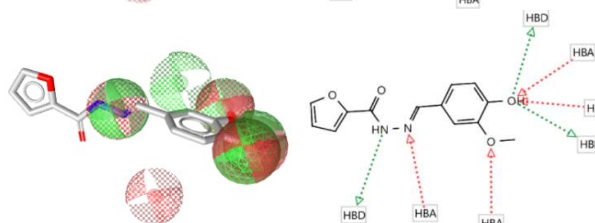
(5) Cysteine



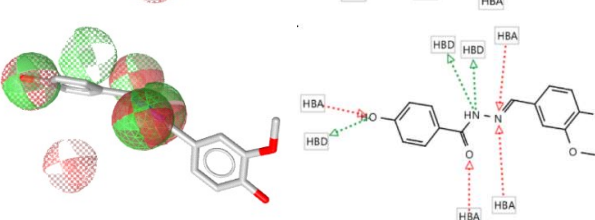
(6) 2-thiophene carboxylic acid hydrazide



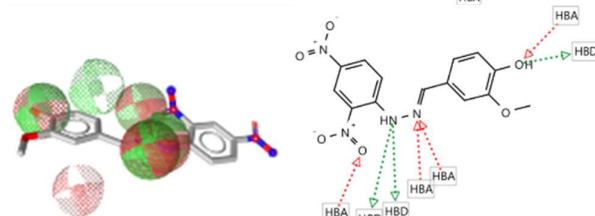
(7) 2-furoic acid hydrazide



(8) 4-hydroxybenzhydrazide

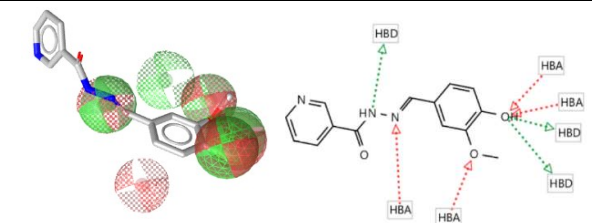


(9) 2,4-dinitrophenylhydrazine

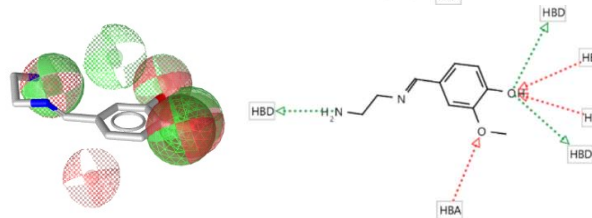




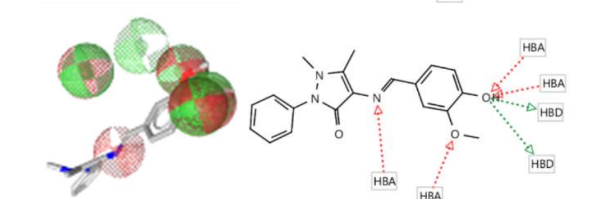
(10) Nicotinic hydrazide



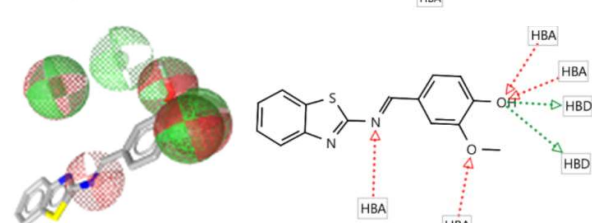
(11) Ethylenediamine



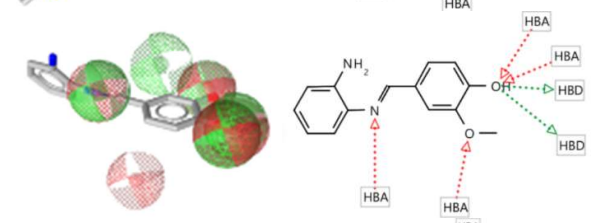
(12) 4-aminoantipyrine



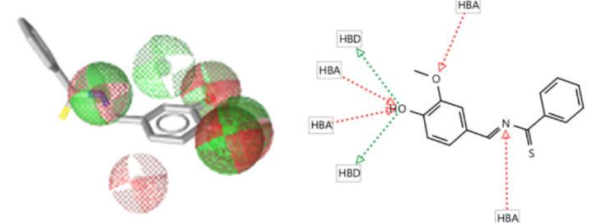
(13) 2-aminobenzothiazole



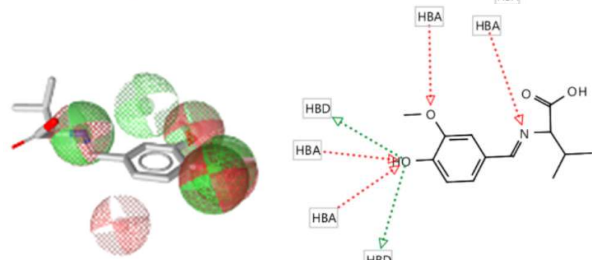
(14) O-phenylenediamine

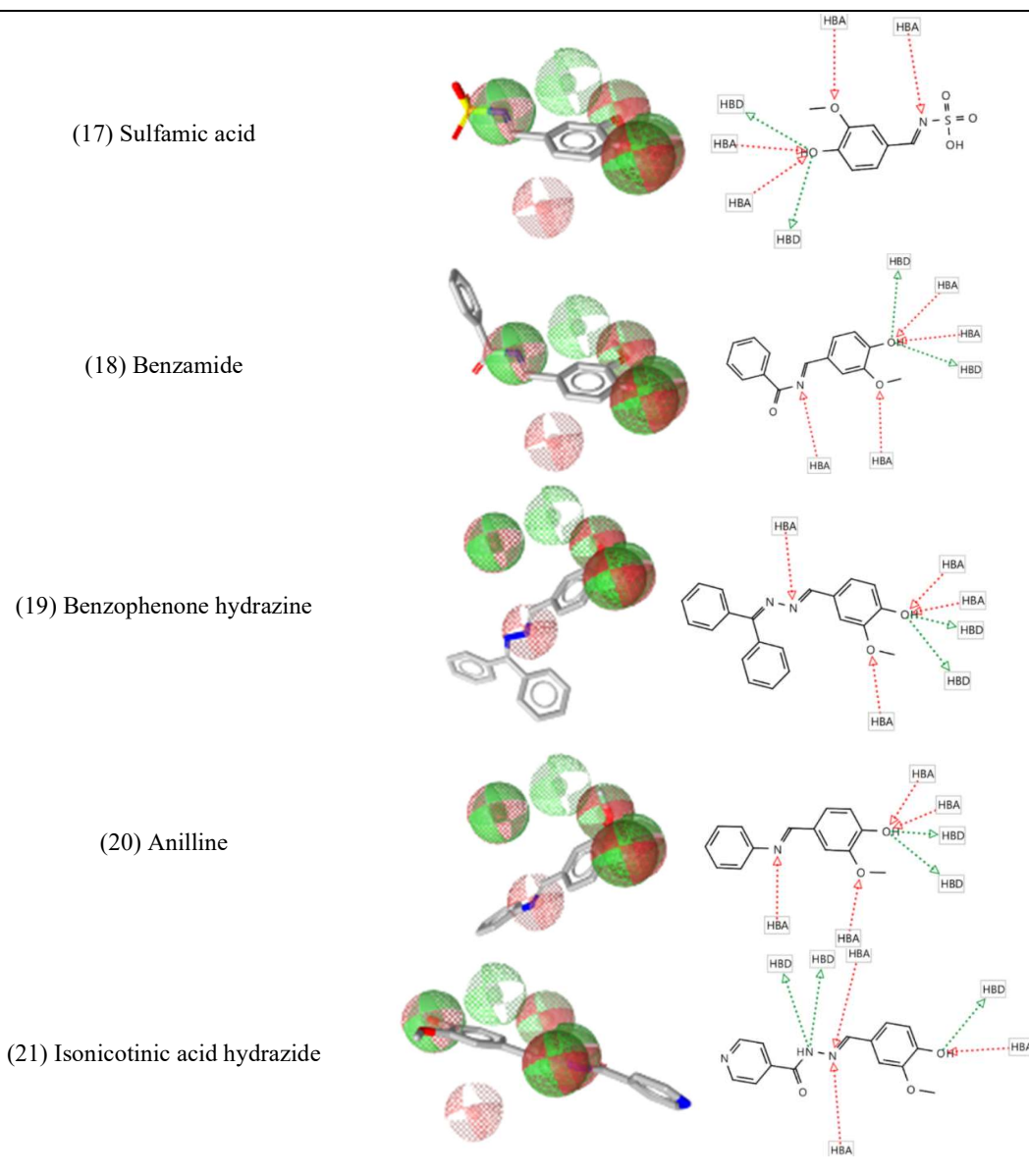


(15) Thiobenzamide



(16) L-Valine





The matching features and pharmacophore fit values shown by the Schiff base vanillin derivatives are based on their functional groups and their molecular orientations. The MMFF94 energies of all Schiff base vanillin derivatives were minimised, thus they depict the most stable orientation. Schiff base vanillin derivatives were derived from a reaction between vanillin and primary amine. HBA and HBD interactions were discovered at the hydroxyl (OH) groups and ether group (C-O-C) of the vanillin part of all derivatives. Therefore, this indicates the importance of vanillin structure in matching with the pharmacophore feature. Vanillin has not only been reported previously for its antibacterial activity against various strains of bacteria, but

also as alternative against multidrug-resistant bacteria (Maisch *et al.*, 2022). This supports the potential inhibitory activity of vanillin against neuraminidase of *Streptococcus pneumoniae*. Secondly, most interactions are shown at the imine linkage (C=N) which is formed between vanillin and primary amine, indicating the significance and potential of Schiff base derivatives as neuraminidase inhibitors of *Streptococcus pneumoniae*. The antibacterial activities of Schiff bases against a variety of bacteria species such as *Staphylococcus aureus*, *Escherichia coli*, *Klebsiella pneumoniae* and *Proteus vulgaris* have been reported, which includes a comparative study as well such that Schiff base ligands showed greater antimicrobial

activity than their respective free ligands (Joseyphus & Nair, 2008). This further supports Schiff base derivatives' potential anti-neuraminidase activity. As for the primary amines which were bonded to the vanillin, most of the interactions are shown at OH group, amino group (NH<sub>2</sub>), nitrogen atom (N), thiol group (SH), and nitro group (NO<sub>2</sub>). Most of the Schiff base vanillin derivatives with high pharmacophore fit values and more matching features have OH groups in the chemical structures, as oxygen atom has lone pairs of electrons to be a potentially good HBA, and hydrogen atom as a good HBD. Vanillin derivatives such as (18), (19), (20) and (21) lack of OH group in their primary amine chemical structure, hence this may result in lower pharmacophore fit values and less matching features. Vanillin derivatives such as (4), (6) and (7), (9) and (10) are still able to show good pharmacophore fit values even without OH group in their primary amine, this may be due to suitable molecular orientation which fits in the pharmacophore model well. Despite the fact that 10 out of 21 Schiff base vanillin derivatives showed good results in ligand-based pharmacophore modelling, the remaining 11 Schiff base vanillin derivatives showed only

slightly less optimal fit value. Thus, all Schiff base vanillin derivatives were subjected to structure-based molecular docking for further analysis and evaluations.

### Pharmacophore Model of Ligand in the Active Site of 2YA8 in Structure-based Molecular Docking

Pharmacophore model of the oseltamivir carboxylate ligand in the active site of 2YA8 is generated to evaluate the interactions of Schiff base vanillin derivatives depicted in the active site of 2YA8. The pharmacophore model generated is composed of 20 pharmacophore features; 2 HBD to active sites HOH2312A and ASP357A, 8 HBA to active sites HOH2499A, HOH2044A, HOH2500A, ARG648A, ARG706A and ARG332A, 5 hydrophobic interactions (HI) to active sites PHE428A, LEU583A, PHE550A, TYR575A and ILE427A, 2 positive ionisable areas (PI) to ASP357A and ASP402A, and 3 negative ionisable areas (NI) to ARG648A, ARG706A and ARG332A. The pharmacophore model is as illustrated in Figure 9, whereas the pharmacophore features to respective active sites in 2YA8 is shown in Figure 10.

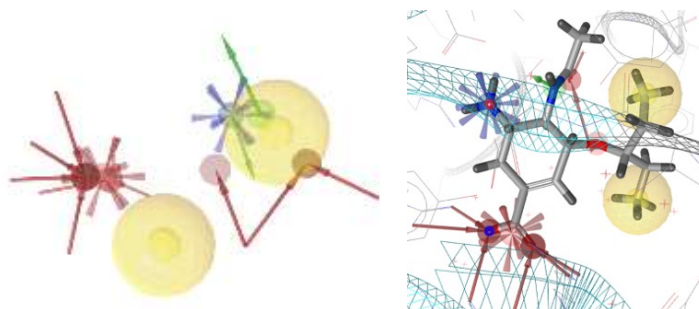


**Figure 9.** Generated pharmacophore model from oseltamivir carboxylate ligand in active site of 2YA8

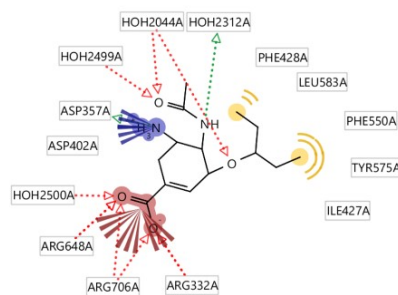


**Figure 10.** Pharmacophore features depicted by oseltamivir carboxylate ligand to respective active sites in 2YA8

### Analysis of Schiff Base Vanillin Derivatives as Potential Neuraminidase Inhibitors of *Streptococcus Pneumoniae* in Structure-based Molecular Docking

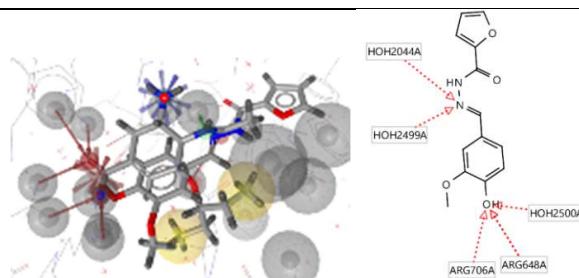
Out of 21 Schiff base vanillin derivatives, only 19 of them successfully aligned with the pharmacophore model of the oseltamivir carboxylate ligand, showing matching

pharmacophore features towards the active sites of 2YA8. Vanillin derivatives (6) and (20) failed to align with the ligand, thus fail to show matching features to interact with the active sites of 2YA8. Table 10 shows the alignment and matching features portrayed by the Schiff base vanillin derivatives to the ligand in 2YA8 active site.

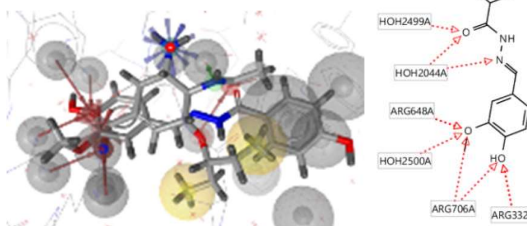
**Table 10.** Alignment and matching features of Schiff base vanillin derivatives to 2YA8 active site

Schiff base vanillin derivatives (Vanillin + ...)	Alignment and matching features
(1) Salicyl hydrazide	
(2) Serine	
(3) Hydrazide hydrate	
(4) Phenylhydrazine	
(5) Cysteine	

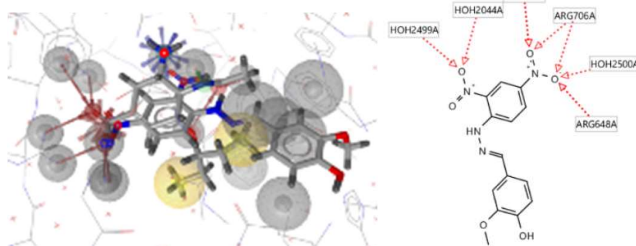
(7) 2-furoic acid hydrazide



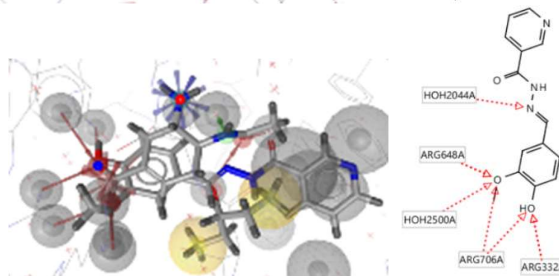
(8) 4-hydroxybenzhydrazide



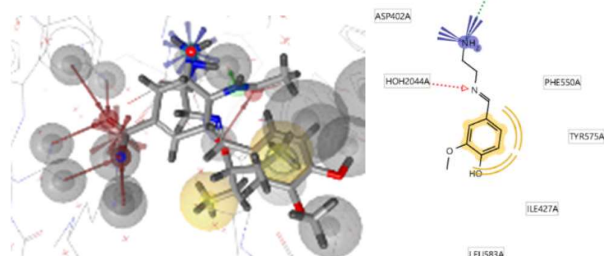
(9) 2,4-dinitrophenylhydrazine



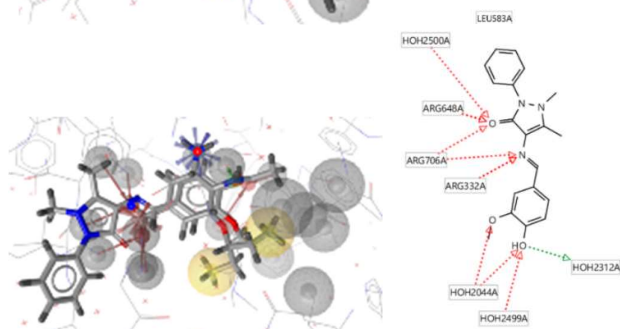
(10) Nicotinic hydrazide



(11) Ethylenediamine

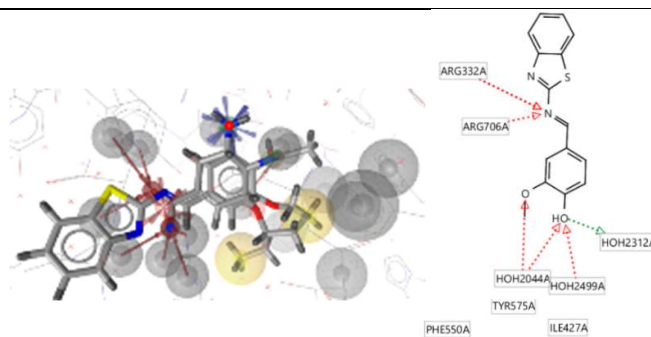


(12) 4-aminoantipyrine

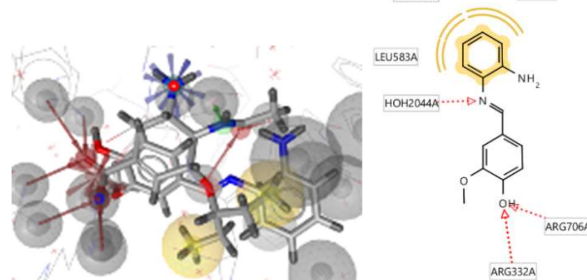




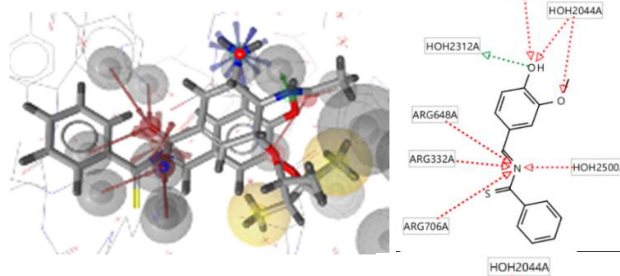
(13) 2-aminobenzothiazole



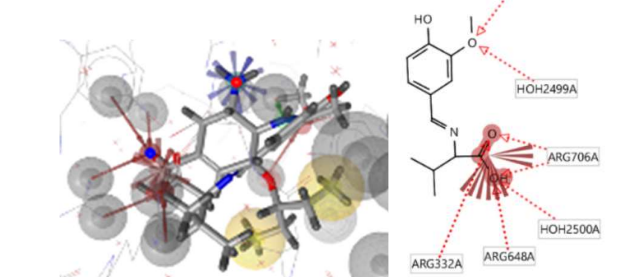
(14) O-phenylenediamine



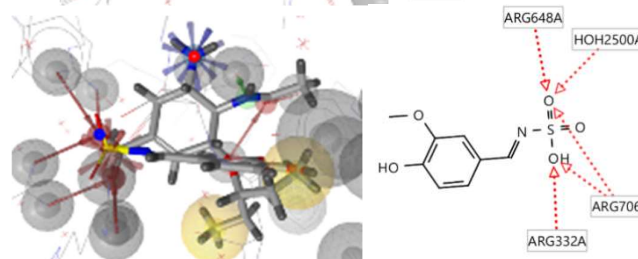
(15) Thiobenzamide

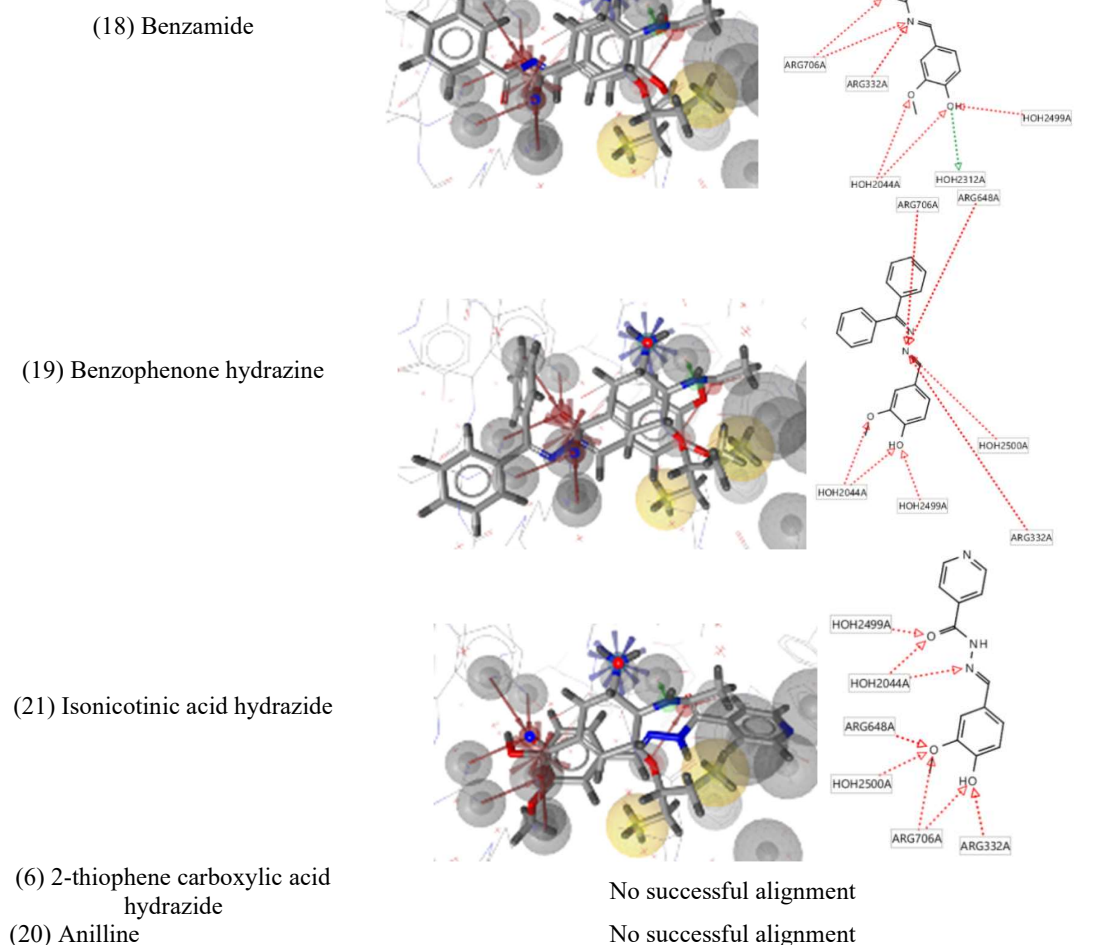


(16) L-Valine



(17) Sulfamic acid





The key active site residues of the catalytic domain in 2YA8 include ARG332, ASP357, GLU632, ARG648, ARG706, and TYR737 (Sharapova *et al.*, 2021). Out of 6 active sites, the Schiff base vanillin derivatives showed interactions towards 4 of them, which include HBA and NI interactions to ARG332, ARG648 and ARG706, as well as HBD and PI interactions to ASP357. In the same protein structure of 2YA8, zanamivir ligand was also reported to show strong binding interaction towards most of the active sites of *Streptococcus pneumoniae* neuraminidase, which include ARG332, ARG648, ARG706 and ASP357 (Sharapova *et al.*, 2021). On top of that, the same bindings are also discovered in the interaction between DANA ligand and the active site of *Streptococcus pneumoniae* neuraminidase (Sharapova *et al.*, 2021). These reported research proved the importance of the active sites in the

evaluation of inhibitory activity against *Streptococcus pneumoniae* neuraminidase, thus further supported the inhibitory potential of the 19 Schiff base vanillin derivatives. Most interactions were depicted at the OH group and C-O-C group of the vanillin part, as well as the C=N linkage between the vanillin and primary amine, giving more fundamental support to the significance of not only Schiff bases, but vanillin as well in inhibitory interaction against *Streptococcus pneumoniae* neuraminidase. As for the primary amines, interactions were mostly shown by NO<sub>2</sub> group, C=O group, benzene ring, carboxylate group (COOH) and sulfonyl group (SO<sub>2</sub>). Despite the fact that most Schiff base vanillin derivatives successfully showed good interaction results towards the active site of 2YA8, other than the molecular formulae of the vanillin derivatives, the structural formulae and molecular orientations are also responsible for

their alignment and matching features to the oseltamivir carboxylate ligand. This may explain the unsuccessful alignment of (6) and (20) to the ligand, as well as failed docking into the active site of 2YA8 even though their chemical structures are similar to the other Schiff base vanillin derivatives. Furthermore, (6) and (20) may also be lack of important functional groups to align with the significant active sites.

### Binding Affinity Values of Schiff Base Vanillin Derivatives

Binding affinity values determine the strength of binding interaction between the Schiff base vanillin derivatives and the active site of 2YA8. The smaller the binding affinity values, the stronger the binding interaction. Being a function of Gibbs free energy, binding affinity values less than -6.00 kcal/mol are considered as active molecules with strong binding interaction (Shityakov & Förster, 2014). Binding affinity values shown by the Schiff base vanillin

derivatives based on the docking outcome are ranged between -6.00 kcal/mol to -7.60 kcal/mol, thus showing strong binding affinity towards the active site of 2YA8. However, (3) was unable to show good binding affinity value, with great probability due to the lack of suitable molecular structure. (3), which is vanillin synthesised with hydrazide hydrate has a water molecule. The water molecule may cause steric hindrance which interfere binding interactions. When water molecule is removed from (3), the Schiff base vanillin derivative of hydrazide was only able to dock with binding affinity value of -5.90. Thus, (3) was unable to show good binding interaction with the pocket of 2YA8, with or without the water molecule. Despite the fact that it is able to align with the oseltamivir carboxylate ligand, the separated chemical structure affects its docking efficiency into the active site of 2YA8. Table 11 summarises the binding affinity values of 18 Schiff base vanillin derivatives towards 2YA8 active site.

**Table 11.** Binding affinity values of Schiff base vanillin derivatives to 2YA8 active site

Schiff base vanillin derivatives (Vanillin + ...)	Binding affinity values (kcal / mol)
(1) Salicyl hydrazide	-7.10
(2) Serine	-6.50
(4) Phenylhydrazine	-7.00
(5) Cysteine	-6.40
(7) 2-furoic acid hydrazide	-7.60
(8) 4-hydroxybenzhydrazide	-6.00
(9) 2,4-dinitrophenylhydrazine	-7.40
(10) Nicotinic hydrazide	-6.60
(11) Ethylenediamine	-6.60
(12) 4-aminoantipyrine	-6.20
(13) 2-aminobenzothiazole	-6.30
(14) O-phenylenediamine	-6.20
(15) Thiobenzamide	-6.10
(16) L-Valine	-6.50
(17) Sulfamic acid	-7.50
(18) Benzamide	-6.50
(19) Benzophenone hydrazine	-6.70
(21) Isonicotinic acid hydrazide	-7.20

### Lipinski's Rule of 5

Lipinski's Rule of 5, or known as RO5, is a rule that is used to evaluate the drugability or druglikeness of chemical compounds, which is their potential as orally active drugs. The evaluation is based on the drug's pharmacokinetics in human body, including their absorption, distribution, metabolism, and excretion (ADME). For a chemical compound to

possess druglikeness, the chemical compound should have no more than 5 HBD, no more than 10 HBA, molecular mass less than 500 g/mol and partition coefficient value less than 5 (Benet *et al.*, 2016). It was concluded that all 18 Schiff base vanillin derivatives fulfilled all the rules in RO5, indicating their potential as promising drug candidates for having druglikeness as orally active drugs. Table 12 summarises the number of HBD, HBA, molecular masses and partition



coefficient values depicted by the 18 Schiff base vanillin derivatives.

**Table 12.** The number of HBD, HBA, molecular masses and partition coefficient values of Schiff base vanillin derivatives

Schiff base vanillin derivatives (Vanillin + ...)	c log P	Hydrogen bond donors (HBD)	Hydrogen bond acceptors (HBA)	Molecular weight (g/mol)
(1) Salicyl hydrazide	1.639	3	5	286.287
(2) Serine	0.265	2	6	239.227
(4) Phenylhydrazine	2.847	2	3	242.278
(5) Cysteine	1.583	2	6	255.292
(7) 2-furoic acid hydrazide	1.526	2	4	260.249
(8) 4-hydroxybenzhydrazide	1.639	3	5	286.287
(9) 2,4-dinitrophenylhydrazine	2.663	2	7	332.272
(10) Nicotinic hydrazide	1.328	2	5	271.276
(11) Ethylenediamine	0.778	2	3	194.234
(12) 4-aminoantipyrine	2.949	1	4	337.379
(13) 2-aminobenzothiazole	3.761	1	4	284.337
(14) O-phenylenediamine	2.734	2	3	242.278
(15) Thiobenzamide	3.195	1	4	271.338
(16) L-Valine	1.929	1	5	251.282
(17) Sulfamic acid	1.703	1	6	231.226
(18) Benzamide	2.428	1	4	255.273
(19) Benzophenone hydrazine	4.272	1	4	330.387
(21) Isonicotinic acid hydrazide	1.328	2	5	271.276

## CONCLUSION

As a whole, out of 21 Schiff base vanillin derivatives, 8 compounds showed potential inhibitory activity against neuraminidase of *Streptococcus pneumoniae* in combination of both results from ligand-based pharmacophore modelling and structure-based molecular docking. These compounds are (1), (2), (4), (5), (7), (8), (9) and (10). 10 out of 21 Schiff base vanillin derivatives, which were compounds (1) to (10) were able to show good pharmacophore fit values of 70 and above and satisfied matching pharmacophore feature with the validated pharmacophore model. On top of that, except for compounds (3), (6) and (20), the remaining 18 Schiff base vanillin derivatives were able to show good docking results in the active site of *Streptococcus pneumoniae* neuraminidase, as well as depicting good alignment with the inhibitory oseltamivir carboxylate ligand in the active site. For showing good binding affinity values and fulfilling Lipinski's Rule of 5 simultaneously, the 8 Schiff base vanillin derivatives were concluded as promising drug candidates opened to be further evaluated for their inhibition activity against *Streptococcus pneumoniae* neuraminidase by other biological assays, including MUNANA assay, which is an assay based on cleavage of neuraminidase on the

2'-(4-methylumbelliferyl)- $\alpha$ -D-N-acetylneuraminic acid.

## ACKNOWLEDGEMENTS

Authors would like to thank MyBrainSc scholarship for all the funding and supports provided. We would also like to express our gratitude towards Faculty of Resource Science and Technology, Universiti Malaysia Sarawak for all the supports, laboratory facilities and computational software provided.

## REFERENCES

- Al-Shar'i, N., & Musleh, S. (2020). Identification of CHK1 Kinase Inhibitors Using Structure-Based Pharmacophore Modelling and Molecular Docking. *Indian Journal of Pharmaceutical Sciences*, 82: 472–482. DOI: 10.36468/pharmaceutical-sciences.670
- Asaruddin, M. R. (2016). *Modelling and Syntheses of Vanillin Derivatives Targeting Influenza Virus Neuraminidase*. (PhD thesis), Universiti Sains Malaysia, Malaysia.
- Benet, L. Z., Hosey, C. M., Ursu, O. & Oprea, T. I. (2016). BDDCS, the Rule of 5 and Drugability. *Advanced Drug Delivery Reviews*, 101: 89–98.

- Benton, D. J., Wharton, S. A., Martin, S. R. & McCauley, J. W. (2017). Role of Neuraminidase in Influenza A(H7N9) Virus Receptor Binding. *Journal of Virology*, 91(11): e02293–16. DOI: 10.1128/jvi.02293-16
- Bogaert, D., de Groot, R. & Hermans, P. W. M. (2004). *Streptococcus Pneumoniae* Colonisation: The Key to Pneumococcal Disease. *The Lancet Infectious Diseases*, 4(3): 144–154. DOI: 10.1016/S1473-3099(04)00938-7
- Centers for Disease Control and Prevention. (2023). *Pneumococcal Vaccination*. Retrieved June 15, 2024, from <https://www.cdc.gov/pneumococcal/vaccines/index.html>
- Centers for Disease Control and Prevention. (2024). *Antibiotic-Resistant Streptococcus Pneumoniae*. Retrieved June 16, 2024, from <https://www.cdc.gov/pneumococcal/php/drug-resistance/index.html>
- Dion, C.F. & Ashurst, J.V. (2022). *Streptococcus Pneumoniae*. Retrieved June 16, 2024 from <https://www.ncbi.nlm.nih.gov/books/NBK470537/>
- European Centre for Disease Prevention and Control. (2023). *Factsheet About Pneumococcal Disease*. Retrieved June 13, 2024, from <https://www.ecdc.europa.eu/en/pneumococcal-disease/facts>
- Grienke, U., Richter, M., Walther, E., Hoffmann, A., Kirchmair, J., Makarov, V., Nietzsche, S., Schmidtke, M. & Rollinger, J. M. (2016). Discovery of Prenylated Flavonoids with Dual Activity Against Influenza Virus and *Streptococcus Pneumoniae*. *Scientific Reports*, 6: 27156. DOI: 10.1038/srep27156
- Guan, S., Zhu, K., Dong, Y., Li, H., Yang, S., Wang, S. & Shan, Y. (2020). Exploration of Binding Mechanism of a Potential *Streptococcus Pneumoniae* Neuraminidase Inhibitor from Herbaceous Plants by Molecular Simulation. *International Journal of Molecular Sciences*, 21(3): 1003. DOI: 10.3390/ijms21031003
- Gut, H., Xu, G., Taylor, G. L. & Walsh, M. A. (2011). Structural Basis for *Streptococcus Pneumoniae* NanA Inhibition by Influenza Antivirals Zanamivir and Oseltamivir Carboxylate. *Journal of Molecular Biology*, 409(4): 496–503. DOI: 10.1016/j.jmb.2011.04.016
- Hsiao, Y. S., Parker, D., Ratner, A. J., Prince, A. & Tong, L. (2009). Crystal Structures of Respiratory Pathogen Neuraminidases. *Biochemical and Biophysical Research Communications*, 380(3): 467–471. DOI: 10.1016/j.bbrc.2009.01.108
- Iyer, U. & Perloff S. (2023). *Pneumococcal Infections (Streptococcus Pneumoniae)*. Medscape. Retrieved June 13, 2024, from <https://emedicine.medscape.com/article/225811-overview>
- Joseyphus, R. S. & Nair, M. S. (2008). Antibacterial and Antifungal Studies on Some Schiff Base Complexes of Zinc(II). *Mycobiology*, 36(2): 93–98. DOI: 10.4489/MYCO.2008.36.2.093
- Li, N., Wang, F., Niu, S., Cao, J., Wu, K., Li, Y., Yin, N., Zhang, X., Zhu, W. & Yin, Y. (2009). Discovery of Novel Inhibitors of *Streptococcus Pneumoniae* Based on the Virtual Screening with the Homology-Modeled Structure of Histidine Kinase (VicK). *BMC Microbiology*, 9(1): 129. DOI: 10.1186/1471-2180-9-129
- Lv, Q., Zhang, P., Quan, P., Cui, M., Liu, T., Yin, Y. & Chi, G. (2020). Quercetin, a Pneumolysin Inhibitor, Protects Mice Against *Streptococcus Pneumoniae* Infection. *Microbial Pathogenesis*, 140: 103934. DOI: 10.1016/j.micpath.2019.103934
- Maisch, N. A., Bereswill, S. & Heimesaat, M. M. (2022). Antibacterial Effects of Vanilla Ingredients Provide Novel Treatment Options for Infections with Multidrug-Resistant Bacteria - A Recent Literature Review. *European Journal of Microbiology & Immunology*, 12(3): 53–62. DOI: 10.1556/1886.2022.00015
- Maragakis, L. L., Perencevich, E. N. & Cosgrove, S. E. (2008). Clinical and Economic Burden of Antimicrobial Resistance. *Expert Review of Anti-Infective Therapy*, 6(5): 751–763. DOI: 10.1586/14787210.6.5.751
- Musher, D. M. (2019). *Streptococcus Pneumoniae*. Haymarket Medical Network. Retrieved June 15, 2024, from <https://www.infectiousdiseaseadvisor.com/ddi/streptococcus-pneumoniae/>
- Nayian, N. A. & Yusof, H. A. (2020). Inhibition of *Streptococcus pneumoniae* Hyaluronidase by Honeys of Malaysian origins. *Bioremediation Science and Technology Research*, 8(1): 1–6.
- Neela, M. M. V. & Peram, S. (2025). Computational Approaches for Drug-Protein Interaction Analysis in Cancer: Machine Learning and Structural

- Bioinformatics Perspectives. Journal of Information Systems Engineering and Management, 10, 231–247. <https://doi.org/10.52783/jisem.v10i10s.1368>
- Nguyen, T. L. A. & Bhattacharya, D. (2022). Antimicrobial Activity of Quercetin: An Approach to Its Mechanistic Principle. *Molecules*, 27(8): 2494. DOI: 10.3390/molecules27082494
- Oliver, F. (2019). *Streptococcus Pneumoniae (pneumococcus): Overview*. News-Medical. Retrieved June 12, 2024, from [https://www.news-medical.net/health/Streptococcus-pneumoniae-\(pneumococcus\)-Overview.aspx](https://www.news-medical.net/health/Streptococcus-pneumoniae-(pneumococcus)-Overview.aspx)
- Owen, C. D., Lukacik, P., Potter, J. A., Sleator, O., Taylor, G. L. & Walsh, M. A. (2015). *Streptococcus Pneumoniae* NanC: Structural Insights into The Specificity and Mechanism of a Sialidase That Produces a Sialidase Inhibitor. *The Journal of Biological Chemistry*, 290(46): 27736–27748. DOI: 10.1074/jbc.M115.673632
- Parker, D., Soong, G., Planet, P., Brower, J., Ratner, A. J. & Prince, A. (2009). The NanA Neuraminidase of *Streptococcus Pneumoniae* is Involved in Biofilm Formation. *Infection and Immunity*, 77(9): 3722–3730. DOI: 10.1128/IAI.00228-09
- Rohani, M. Y., Raudzah, A., Ng, A. J., Ng, P. P., Zaidatul, A. A., Asmah, I., Murtaza, M., Parasakthy, N., Mohd Yasmin, M. Y. & Cheong, Y. M. (1999). Epidemiology of *Streptococcus Pneumoniae* Infection in Malaysia. *Epidemiology and Infection*, 122(1): 77–82. DOI: 10.1017/s0950268898001605
- Sharapova, Y., Suplatov, D. & Švedas, V. (2018). Neuraminidase A from *Streptococcus Pneumoniae* Has a Modular Organization of Catalytic and Lectin Domains Separated by a Flexible Linker. *The FEBS Journal*, 285(13): 2428–2445. DOI: 10.1111/febs.14486
- Sharapova, Y., Švedas, V. & Suplatov, D. (2021). Catalytic and Lectin Domains in Neuraminidase A from *Streptococcus Pneumoniae* are Capable of an Intermolecular Assembly: Implications for Biofilm Formation. *The FEBS Journal*, 288: 3217–3230. DOI: 10.1111/febs.15610
- Shityakov, S. & Förster, C. (2014). *In Silico* Predictive Model to Determine Vector-Mediated Transport Properties for the Blood-Brain Barrier Choline Transporter. *Advances and Applications in Bioinformatics and Chemistry*, 7: 23–36. DOI: 10.2147/AABC.S63749
- Syed, S., Hakala, P., Singh, A. K., Lapatto, H. A. K., King, S. J., Meri, S., Jokiranta, T. S. & Haapasalo, K. (2019). Role of Pneumococcal NanA Neuraminidase Activity in Peripheral Blood. *Frontiers in Cellular and Infection Microbiology*, 9: 218. DOI: 10.3389/fcimb.2019.00218
- Walther, E., Richter, M., Xu, Z., Kramer, C., von Grafenstein, S., Kirchmair, J., Grienke, U., Rollinger, J. M., Liedl, K. R., Slevogt, H., Sauerbrei, A., Saluz, H. P., Pfister, W. & Schmidtke, M. (2015). Antipneumococcal Activity of Neuraminidase Inhibiting Artocarpin. *International Journal of Medical Microbiology*. 305(3): 289–297. DOI: 10.1016/j.ijmm.2014.12.004
- World Health Organization. (2022). *Pneumonia in Children*. Retrieved June 12, 2024, from <https://www.who.int/news-room/fact-sheets/detail/pneumonia>
- Xu, L., Fang, J., Ou, D., Xu, J., Deng, X., Chi, G., Feng, H. & Wang, J. (2023). Therapeutic Potential of Kaempferol on *Streptococcus Pneumoniae* Infection. *Microbes and Infection*, 25(3): 105058. DOI: 10.1016/j.micinf.2022.105058